This manuscript is a non-peer reviewed preprint submitted to EarthArXiv.
The manuscript has been submitted to The Depositional Record and is currently under consideration. As a function of the peer-reviewed process, the contents of the manuscript may change. If accepted, the final version of this manuscript will be available via the 'Peer-reviewed Publication DOI' link on the right-hand side of this webpage.

Water discharge and sediment flux intermittency in the fluvial Escanilla Formation, Spain: Implications for changes in stratigraphic architecture

Nikhil Sharma[1], Alexander C. Whittaker[2], Thierry Adatte[3], Sébastien Castelltort[1]

[1]Department of Earth Sciences, University of Geneva, Rue des Maraichers 13, 1205 Geneva, Switzerland

[2]Department of Earth Science and Engineering, Imperial College London, South Kensington, London SW7 2AZ, England

[3]Institute of Earth Sciences, University of Lausanne, Géopolis, 1015 Lausanne, Switzerland

ABSTRACT

Water discharge and sediment flux variations are important parameters controlling the morphodynamical behavior of rivers. Although quantitative estimates for discharge and flux variability are well constrained for modern rivers, far fewer assessments of flow and sediment flux intermittency in ancient fluvial systems from the rock record are available. In this study we explore the relationship between water discharge, sediment flux variability and patterns of changing fluvial stratigraphic architecture in the Middle Eocene Escanilla Formation, Spain. We estimate water discharge intermittency factor (I_{WF}) to range from 0.03 – 0.11 in the HA intervals and from 0.10 – 0.32 in the LA intervals. Sediment flux intermittency factor (I_{SF}) is in the range of 0.008 – 0.01 in the HA intervals and from 0.01 – 0.03 in the LA intervals. Consequently, we suggest that high amalgamation (HA) intervals were most likely deposited under more intermittent and short-lived intense precipitation events, while low amalgamation (LA) intervals were the result of less intermittent flows spread throughout the year. Overall, our estimates are consistent with values from modern ephemeral rivers typically found in arid to semi-arid climatic conditions, which is in agreement with available proxy data for the Middle Eocene climatic context of the studied alluvial system. Our data highlights the important connection between hydroclimate, river morphodynamics and landscape evolution, and has implications to predict river flow and sediment transport across the Earth's surface in the geological past.

Keywords: Middle Eocene, Escanilla Formation, paleohydraulics, intermittency

INTRODUCTION

The response of river systems to changing hydroclimates is of increasing importance for predicting floods hazards and its impact on growing urbanization in the context of global climate perturbations. Water discharge (hereafter referred to as "discharge") and sediment flux (hereafter referred to as "flux") in rivers are correlated to mean annual precipitation, which is linked to prevalent climatic conditions [Langbein and Schumm, 1958; Syvitski and Milliman, 2007;

Hansford et al., 2020]. However, rivers in semi-arid to subhumid tropics display a wide range of discharge variability depending on the balance between precipitation and evapotranspiration with many rivers showing pronounced runoff seasonality and inter-annual variability [Alexander et al., 1999; Fielding et al., 2009, 2011, 2018]. Discharge and flux variability are further important as they can play a key role in controlling landscape evolution and the consequent sedimentary record of rivers [e.g., Allen et al., 2013; Plink-Bjorklund, 2015, 2017; Fielding et al., 2018; Hansford et al., 2019, 2020; Lyster et al., 2022]. Seasonal discharge variability, in particular, has been found to influence preserved stratigraphy and sedimentology and thus plays an important role in the construction of fluvial bodies both in ancient and modern environments [Fielding et al., 2018; Lyster et al., 2022]. Discharge variability is also crucial to bedrock rivers through its role in controlling bedrock river incision and continental erosion thereby driving the resulting flux of sediments into depositional basins [Lague et al., 2005 and references therein].

Sediment flux, depending on grain size, in rivers is typically more intermittent than discharge variation [Allemand et al., 2023]. For instance, bedload sediments are typically transported only during floods when there is enough shear stress for such sediments to be entrained and transported [Phillips and Jerolmack, 2014; Phillips et al., 2018; Allemand et al., 2023]. The frequency of discharge events and quantity of sediment transported is thus an important parameter to assess the efficiency of sediment transport, and the ability of fluvial systems to convey environmental signals from sources to sinks in both modern and ancient systems [e.g., Castelltort and Van den Driessche, 2003; Armitage et al., 2011; Simpson and Castelltort, 2012; Romans et al., 2016; Tofelde et al., 2021].

Modern river streamflow conditions are typically described in terms of the presence or duration of flow and are a fundamental metric in classifying rivers as perennial and non-perennial (intermittent and ephemeral) [e.g., Poff, 1996; Bond et al., 2010; Eng et al., 2015; Sauquet et al., 2021]. Further, climate plays a primary role in influencing streamflow patterns, in addition to other factors such as topography and vegetation [e.g., Beaufort et al., 2019], such that the more arid the climate, higher is the probability of a fluvial system to be non-perennial [e.g., Sauquet et al., 2021]. While changes in flow patterns in modern rivers can be easily recorded using gauging stations, there exist currently few studies, such as e.g., Hayden et al, (2021), which explicitly quantify flow variability or intermittency in the rock record.

Simply put, the temporal distribution of flow and sediment transport in a river is referred to as its intermittency. Two extreme cases can be identified: a highly intermittent system is characterized by repeated or prolonged intervals of no flow or sediment transport, while a non-intermittent system is characterized by continuous flow or sediment transport [Lyster et al., 2022]. To study sediment fluxes and basin infilling over extended geological timeframes, Paola et al. (1992) introduced a dimensionless intermittency factor ranging from zero to one. This factor serves as a means of scaling instantaneous sediment transport rates to longer term sediment fluxes or depositional volumes in geological applications. The chosen averaging time should be considerably longer than individual channel-forming events (instantaneous conditions), yet relatively shorter than the overall geological timescale (mean conditions). The most straightforward approach is to assume that flow is intermittently characterized by a sequence of bankfull channel-forming conditions [Paola et al., 1992]. Consequently, discharge or flux intermittency factor can be calculated relative to a longer timescale, such as the number of days in a year. For instance, an intermittency of 120 days yields an intermittency factor of 0.33 or 33 % of a year. The intermittency factor therefore corresponds to the cumulative occurrence of these channel-forming conditions and is precisely described as the proportion of a selected time interval necessary for a constant channel-forming flow to transport an equivalent amount of water or sediment as the river hydrograph accomplishes during that time period [Paola et al., 1992]. The lower the intermittency factor, the more intermittent the 5ischarge or flux is relative to annual or longer-term measures of water and sediment budget.

In this study, we for the first time explore a potential relationship between observed changes in fluvial stratigraphic architecture in the Escanilla Formation, Spain, and river discharge and flux variability that we have reconstructed from the sedimentary record. To perform such a quantitative assessment, we estimated discharge and flux intermittency and their respective intermittency factors. We further compare intermittency factors to those from modern rivers and classify the Middle Eocene Escanilla rivers as either perennial or non-perennial and collectively discuss these results within the framework of the observed stratigraphic changes, the paleo-hydroclimate context, and implications for interpreting changes in fluvial stacking patterns recorded in alluvial sedimentary successions.

GEOLOGICAL BACKGROUND

The Escanilla sediment routing system

The Escanilla sediment routing system, located in the Pyrenees, is preserved sediment routing system, of mid- to late Eocene age (ca. 41 – 34 Ma), that linked catchment regions of the high Pyrenees, via the Sis- and Gurb paleovalleys, to depositional sinks in the south Pyrenean foreland Basin (Fig. 1) [Bentham et al., 1993; Labourdette & Jones 2007; Labourdette 2011; Michael et al., 2013]. Extensive paleocurrent data suggests that these two paleovalley systems sourced sediments from the axial zone of the Pyrenees with a confluence of these two systems in the Viacamp area (Fig. 1). From there sediments were transported downstream towards the west, via the Ainsa Basin [Vincent 2001; Whittaker et al., 2011; Parsons et al., 2012; Michael et al., 2013], (Fig. 1). The entire Escanilla sediment routing system has been extensively mapped within a single source-to-sink framework through a range of provenance tools such as clast lithologies, heavy minerals, U–Pb geochronology of detrital zircons, apatite fission track analysis, paleocurrent analysis, magneto- and biostratigraphy, and has been explained in detail by Michael et al. (2013, 2014b) and references therein.

The Escanilla Formation at Olson – fining upward sequences

Within the southern Ainsa Basin, the Escanilla Formation has a maximum preserved thickness of ~1000 m and is divided into the Mondot and Olson Members [Bentham et al., 1992, 1993; Dreyer et al., 1992; Kjemperud et al., 2004; Labourdette and Jones 2007; Labourdette 2011]. Previously, several stratigraphic sequences consisting of laterally amalgamated and vertically stacked channels have been described by Labourdette and Jones (2007), and Labourdette (2011). This study focuses on 3 fining-upward sequences at Olson, recently described by Sharma et al., (2023), with each sequence having a thickness around 35 – 45 m. Each fining-upward sequence consists of a high amalgamation (HA) interval which is defined as a 5 to 12 m thick and 600 to 2000 m wide complex of laterally and vertically amalgamated channel bodies in multiple stories, and a low amalgamation (LA) interval which is defined as a floodplain-dominated interval consisting of isolated channel bodies (less amalgamated) that are 2 to 4 m thick and 100 to 500 m wide [Sharma et al., 2023]. Recent work in the Middle Eocene fluvial Escanilla Formation, Spain, has documented cyclical variations in instantaneous water discharge and bedload sediment flux relative to changes in stratigraphic architecture, i.e., from high amalgamation (HA) to low amalgamation (LA) intervals within several fining upward sequences is indicative of an upstream climate control on fluvial stacking pattern [Sharma et al., 2023].

Regional climate during the Middle Eocene

The Escanilla Formation at Olson encompasses the Middle Eocene Climatic Optimum (MECO), a global warming event at ~ 40 Ma. Geochemical proxies from the Escanilla Formation suggest regional climatic conditions in the south-central Pyrenees to be dry, arid, and devoid of much vegetation [Sharma et al., 2023]. In other localities more to the East of the Ebro Basin, (northeastern Spain), other proxies such as palynological, pollen taxa and floral diversity [Cavagnetto and Anadón 1996; Haseldonckx, 1972] suggest warm and humid climatic conditions. For instance, Middle Bartonian vegetation from the eastern Ebro basin was characterized by a diverse mangrove swamp-type vegetation along the coast which subsequently disappeared by the Priabonian [Cavagnetto and Anadón 1996]. Such differences in regional climate could be due to a phase of climate transitioning, expressed differently in different regions, from a warm tropical Early Eocene Climatic Optimum to a colder and arid early Oligocene [López-Blanco et al., 2000; Cantalejo et al., 2015]. Collectively, this makes the Escanilla Formation at Olson an ideal locality to test for the link between discharge, transport intermittency and different stratigraphic stacking patterns and architecture under greenhouse conditions of the Middle Eocene.

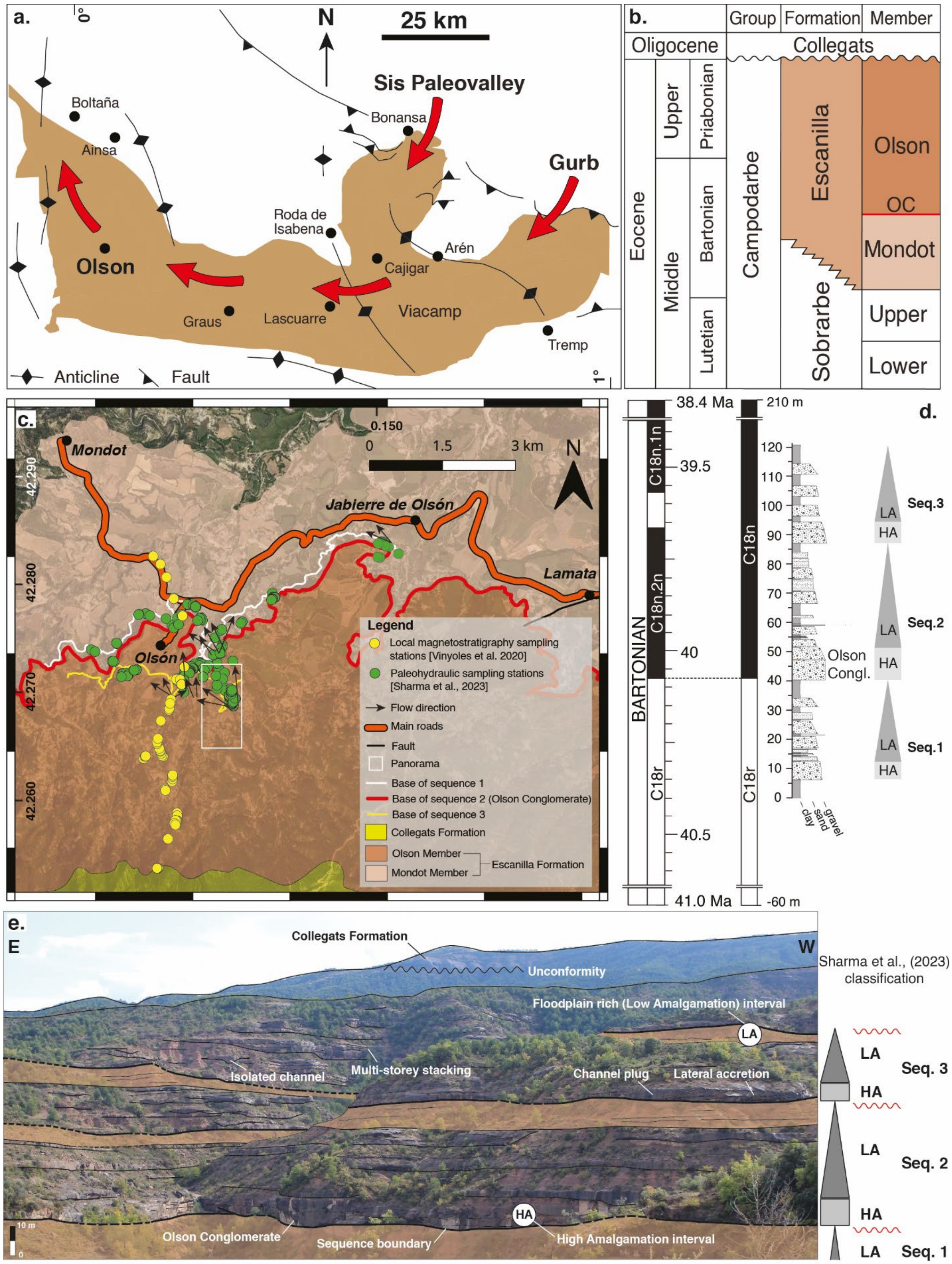

a.
0°
N
25 km
Sis Paleovalley
Gurb
Boltaña
Ainsa
Bonansa
Roda de Isabena
Arén
Cajigar
Olson
Graus
Lascuarre
Viacamp
Tremp
1°
Anticline
Fault
b.
Group
Formation
Member
Oligocene
Collegats
Eocene
Upper
Middle
Priabonian
Bartonian
Lutetian
Campodarbe
Escanilla
Sobrarbe
Olson
OC
Mondot
Upper
Lower
c.
0.150
0
1.5
3 km
N
Mondot
Jabierre de Olsón
Lamata
Olsón
42.290
42.280
42.270
42.260
Legend
Local magnetostratigraphy sampling stations [Vinyoles et al. 2020]
Paleohydraulic sampling stations [Sharma et al., 2023]
Flow direction
Main roads
Fault
Panorama
Base of sequence 1
Base of sequence 2 (Olson Conglomerate)
Base of sequence 3
Collegats Formation
Olson Member
Mondot Member
Escanilla Formation
d.
38.4 Ma
39.5
40
40.5
41.0 Ma
C18n.1n
C18n.2n
C18r
BARTONIAN
210 m
C18n
C18r
-60 m
120
110
100
90
80
70
60
50
40
30
20
10
0
clay
sand
gravel
Olson Congl.
LA
HA
Seq.3
Seq.2
Seq.1
e.
E
W
Collegats Formation
Unconformity
Floodplain rich (Low Amalgamation) interval
Isolated channel
Multi-storey stacking
Channel plug
Lateral accretion
Olson Conglomerate
Sequence boundary
High Amalgamation interval
10 m
0
Sharma et al., (2023) classification
LA
HA
Seq. 3
Seq. 2
Seq. 1

Figure 1. (a) Map of the Escanilla paleo-sediment routing system in the southern Pyrenees, Spain, and showing the main tectonic structures. Figure modified after Michael et al. (2014a). Red arrows mark the water discharge and sediment transport direction of the Escanilla system away from the source regions of Sis- and Gurb paleovalleys. (b) Lithostratigraphic framework of the Escanilla Fm at Olson consists of two main Members – the Mondot and the Olson Member with the Olson Conglomerate (OC; red line) at the transition between the two Members. (c) Geological map of the southern Ainsa basin encompassing the Escanilla Formation around the village of Olson. The 'Olson Conglomerate (OC)' is marked in red as a basin wide, laterally extensive amalgamated channel body lying in-between the Mondot and Olson Members of the Escanilla Formation. This map was prepared using QGIS Desktop 3.22.8 (https:// qgis. Org/ en/ site/). (d) Studied composite section of the Escanilla Fm with the local magnetostratigraphic interpretation by Vinyoles et al. (2020) correlated to the Geomagnetic Polarity Time Scale (GPTS 2020) [Ogg, 2020]. The 90 thickest normal magnetozone C18n in the local magnetostratigraphic interpretation includes C18n.1n, C18n.1r, and C18n.2n. I Panorama of the studied sequences 2, and 3 (sequence 1 lies below). At the base of the panorama lies a thick floodplain dominated interval terminating the LA interval of sequence 1, and above which lies the high amalgamation (HA) interval corresponding to the OC. Above the HA interval lies the floodplain dominated low amalgamation (LA) interval.

METHODS

The concept of discharge intermittency can most simply be expressed through a discharge intermittency factor (I_{WF}) which has been defined by Paola et al., (1992) as:

$$I_{WF} = \frac{\Sigma Q_w}{Q_{w(cf)} \Sigma t} \tag{1}$$

Where, Q_w is the total water discharge over the averaging time period, such as a year, $Q_{w(cf)}$ is the instantaneous channel-forming water discharge, and Σt is the averaging time period (e.g., 1 year). Following Eq. 1, flux intermittency factor (I_{SF}) can be expressed as:

$$I_{SF} = \frac{\Sigma Q_s}{Q_{s(cf)} \Sigma t} \tag{2}$$

Where, Q_s is the total sediment flux over the period of interest and $Q_{s(cf)}$ is the instantaneous channel forming sediment flux. Σt is the timespan equal to 1 year [Paola et al., 1992].

These calculations require estimates for both channel forming discharges and longer-term water budgets, and similarly, sediment transport capacities and longer-term sediment flux rates. For instantaneous discharge and flux conditions in the Escanilla Formation we use the recently published palaeohydrological reconstructions for the HA and LA units of Sharma et al., (2023), which are based on field measurements of channel geometries and sediment caliber. However, drainage area, precipitation, and total volumetric sediment flux estimates are required to approximately estimate the total water and sediment budget available to the Escanilla system.

Drainage area estimates

Catchment area of ancient sediment routing systems are often hard to accurately constrain due to tectonic changes and erosion of the hinterland [Eide et al., 2018; Brewer et al., 2021]. However, the Escanilla system's source area is relatively well-constrained: A total drainage area upstream of Olson, based on the mapping of the Escanilla system by Michael et al. (2014a), was estimated to be in the range of 2500 – 5500 km^2 with an average value of approximately 4000 km^2. This estimate is similar to that proposed by Brewer et al., (2021) for the Escanilla system. The value includes a combined average area of approximately 2050 km^2 from the Sis and Gurb catchment areas (2088 km^2 is suggested by Michael et al. (2014a)) while the downstream region until Olson constitutes an area of approximately 1950 km^2.

Total water budget and water discharge estimates

Total water budget

Total water budget for the Escanilla Fm was estimated using two end members of mean annual precipitation rates (~0.3 m yr^{-1} and ~1.0 m yr^{-1}). In the first instance, Sharma et al., 2023 estimated mean annual precipitation (MAP) (Fig. 2), using the chemical index of weathering (CIW) of paleosol samples from the Escanilla Formation, which gave values ranging between 0.25 m yr^{-1} and 0.57 m yr^{-1} (average value of 0.33 m yr^{-1}). It is important to note here that these MAP values are based only on samples from the LA interval due to the absence of floodplain in the HA intervals. Multiplying average total drainage area of 4000 km^2 by average mean rainfall results in an average total water budget of $13x10^8$ m^3 yr^{-1} with minimum and maximum values of $7x10^8$ m^3 yr^{-1} and $31x10^8$ m^3 yr^{-1} respectively. These values are maxima because they do not include water loss due to infiltration or evapotranspiration but are reasonable first-order estimates.

In the second instance, Eocene MAP estimates for northern Spain predicted by Tardif et al. (2021) can be used to estimate the total water budget. These MAP estimates are in the range of 0.8 m yr^{-1} to 1.4 m yr^{-1} with an average value of 1.1 m yr^{-1} equivalent to an average total water budget of $4x10^9$ m yr^{-1} with minimum and maximum values of $2x10^9$ m yr^{-1} and $7x10^9$ m yr^{-1} respectively.

Water discharge estimates

Detailed water discharge, in m^3 s^{-1}, for the three sequences at Olson was estimated by Sharma et al., (2023), using a combination of channel dimensions such as bankfull depth and width, and paleoslope estimates (Fig. 2). HA intervals have an average discharge rate of 2200 ± 550 [m^3 s^{-1}] (average value ± standard error, N = 45) in HA intervals, and a discharge rate of 700 ± 200 [m^3 s^{-1}] (N = 49) in the LA intervals which corresponds to a 3-fold increase of volumetric discharge during HA intervals. However, it is important to note that these estimates represent instantaneous bank full flow conditions (channel forming conditions) and do not represent average annual flow conditions.

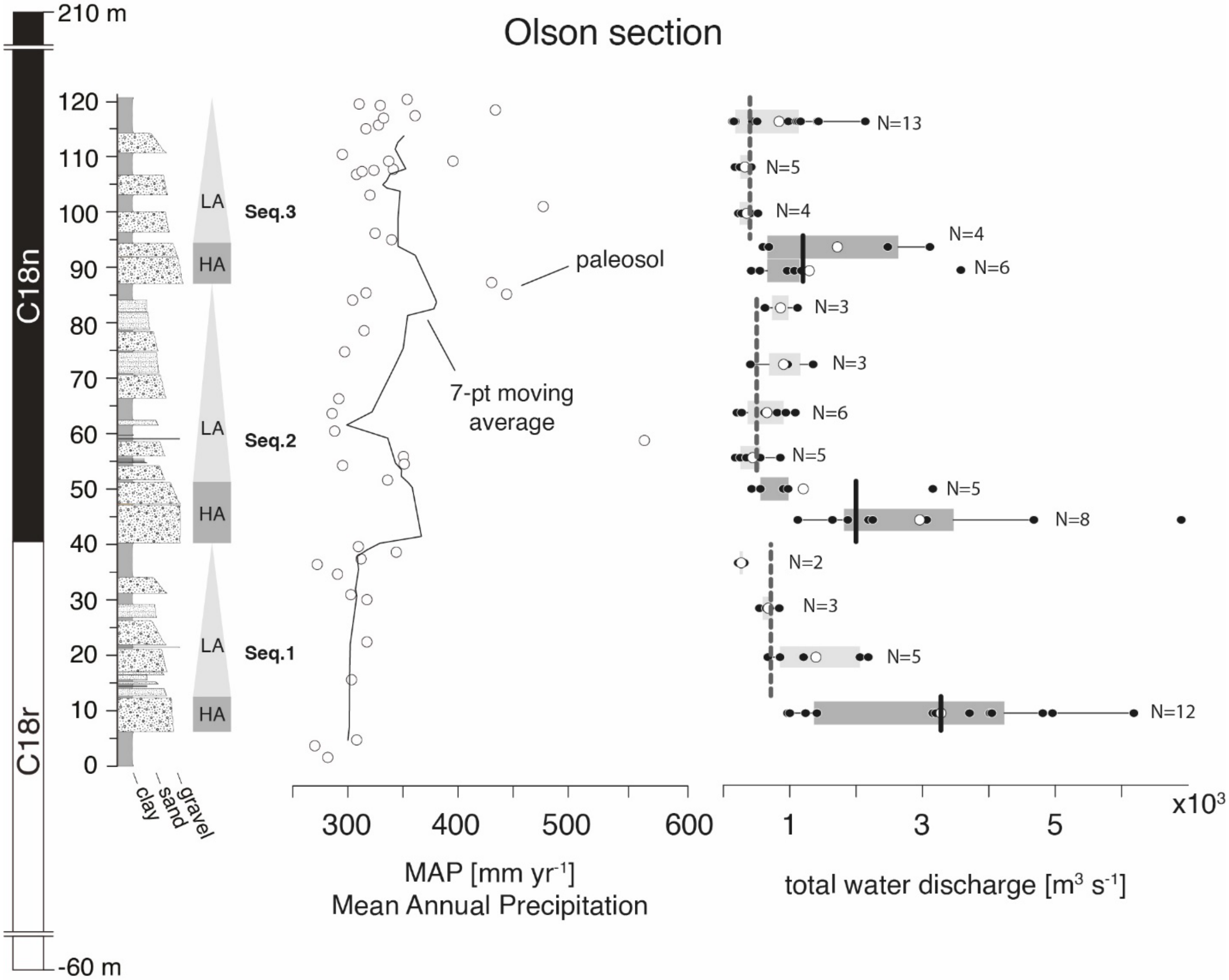

Figure 2. Stratigraphic log of the studied section at Olson and depicting the three fining upward sequences, each consisting of a high amalgamation (HA) and low amalgamation (LA) interval. Also shown are the mean annual precipitation (MAP) and total water discharge estimates for the Escanilla Formation. Black vertical bars denote the average value in HA intervals while grey bars denote the average value in LA intervals.

Estimating discharge intermittency factor

Discharge estimates, in $m^3 s^{-1}$, for the three sequences at Olson from both end members, were first converted into $m^3 day^{-1}$. Discharge intermittency (Q_{WI}) was then calculated by dividing the average total available water budget by discharge estimates in $m^3 day^{-1}$ to obtain the intermittency ratio as the number of days per year that channel forming discharge would be required to equal the estimated annual water budget. Discharge intermittency factor (I_{WF}) was calculated relative to the number of days in a year.

Total sediment budget and sediment flux estimates

Bankfull volumetric sediment flux and the resulting total sediment flux for the Escanilla Formation was calculated using two different approaches involving bedload and sand-fraction sediment flux estimates.

Total sediment budget

The total volumetric sediment flux available in the Escanilla system during the 41.6 – 39.1 Ma time interval has previously been estimated by Michael et al. (2013) using an approach extrapolating the outcrop extent of the sediment routing system, where linear interpolation of cross-sectional areas in the downstream direction is used to constrain the cumulative depositional volume. The most significant uncertainty acknowledged by Michael et al. (2013) arises from the estimated cross-sectional width of the Escanilla system fairway. This mass balance framework resulted in a total depositional volume of 246000 ± 20000 $m^3 yr^{-1}$, a value range which we use for this study.

Estimating bedload sediment flux and resulting total sediment flux

Bedload sediment flux for the gravel grain size fraction was estimated by Sharma et al., 2023 (Fig. 4). Since gravel fraction makes up 25 % of the total sediment flux in the Ainsa area of the Escanilla system in the Ainsa Basin, as documented by Michael et al. (2013) using a modelling approach involving transformation of volumetric depositional volumes into a mass balance framework, bedload sediment flux was accordingly used to calculate the total sediment flux.

Estimating sand-fraction sediment flux and resulting total sediment flux

Sand-fraction sediment flux was estimated using the model of Engelund and Hansen (1967). Non-dimensional sediment flux per unit width (q_t^*) was calculated as:

$$q_t^* = \left(0.05/C_f\right) \times (\tau_*)^{2.5} \tag{1}$$

Where C_f is the friction factor and is calculated as:

$$C_f = \left(gH_{bf}S\right)/U^2 \tag{2}$$

Where g is gravitational acceleration, H_{bf} is bankfull flow depth, S is riverbed slope and U is flow velocity. These values have been previously estimated for the Escanilla Formation by Sharma et al., (2023).

Using the model of Engelund and Hansen (1967), total nondimensional shear stress (τ_*) is related to bankfull flow depth (H_{bf}), slope (S), submerged specific sediment density (R = 1.65 for quartz in water) and median grain size (D_{50}) as:

$$\tau_* = \left(H_{bf}S\right)/(RD_{50}) \tag{3}$$

Since, $q_t^* = Q_s/W(RgD_{50}^3)^{0.5}$ [Engelund and Hansen, 1967], Bankfull sediment flux (Q_s) was then calculated using Eq. 4 as:

$$Q_s = q_t^* \times W \times (RgD_{50})^{0.5} \tag{4}$$

Where W is the flow width. A median grain size of 0.25 mm (fine-medium grain size fraction) was considered while calculating the sand-fraction sediment flux. Channel-belt widths estimated by Sharma et al. (2023), using the relationship $W = 8.8H_{bf}^{1.82}$ [Bridge and Mackey, 1993], where used to calculate Bankfull sediment flux (Q_s). Similar to the gravel fraction, sand-fraction also makes up 25 % of the total sediment flux [Michael et al., 2013] and values were accordingly used to calculate the resulting total sediment flux in the Ainsa Basin.

Estimating sediment flux intermittency factor

Total sediment flux estimates, in m^3 s^{-1}, from both approaches (bedload- and sand-fraction) were first converted into m^3 day^{-1}. Flux intermittency (Q_{SI}) for each approach was then obtained by dividing the total available annual sediment budget by the sediment flux in m^3 day^{-1} to obtain the flux intermittency, expressed in terms of the number of days in a year. Flux intermittency factor (I_{SF}) was then estimated using the same approach used to estimate discharge intermittency factor. Uncertainty on all results reported in this study consist of the standard error of the mean (SE) calculated as $SE = \frac{SD}{\sqrt{n}}$, where SD is the standard deviation and n is sample size. Uncertainty propagation was carried out using the uncertainties package on Python (Spyder version 4.0.1), which is a free, cross-platform program that transparently handles calculations with numbers involving uncertainties.

RESULTS

Water discharge intermittency factor (I_{WF})

Bankfull water discharge intermittency, estimated using the first end member (~0.3 m yr^{-1} MAP), in the HA intervals is 12 ± 2 days (average value ± standard error, N = 35), equivalent to an intermittency factor of 0.03 or 3 % of a year, while LA intervals have an intermittency of 39 ± 4 days (N = 49), equivalent to an intermittency factor of 0.10 or 10 % of a year and represent a 3-fold increase in intermittency factor in the LA intervals over HA intervals (Fig. 3), again noting that an increase in the numerical value of the intermittency factor (I_{WF}) implies a decrease in the temporal intermittency of water discharge – i.e., water flow is relatively more constant through the year in the LA intervals.

Discharge intermittency, based on the second end member (~1.0 m yr^{-1} MAP), in the HA intervals is 40 ± 5 days (N = 35), equivalent to an intermittency factor of 0.11 or 11 % of a year, while LA intervals have an intermittency of 119 ± 13 days (N = 47), equivalent to an intermittency factor of 0.32 or 32 % of a year and represents an almost 3-fold increase in discharge intermittency factor. Overall, discharge intermittency values from both end-members suggest that flow during HA intervals was more intermittent (likely concentrated within a few days in a year) while flow during LA intervals was less intermittent and more likely to be characterized by non-bankfull perennial flow. Any increase in precipitation in the source area would result in a higher water budget translating overall into a higher discharge intermittency factor (I_{WF}), i.e., less intermittent flow. The Escanilla system is consistent with lower discharge intermittency in temporal sense under increased precipitation and supports evidence from modern rivers that climatic conditions such as the amount and timing of precipitation have a first-order control on flow variability [e.g., Buttle et al., 2012; Eng et al., 2015]. In contrast higher flow intermittencies (i.e., a few days a year) in HA intervals more typical of ephemeral (intermittent) streams where flows are typically short, intense, and associated with periods of intense rainfall [e.g., Piccard and High, 1973; Mabbut, 1977].

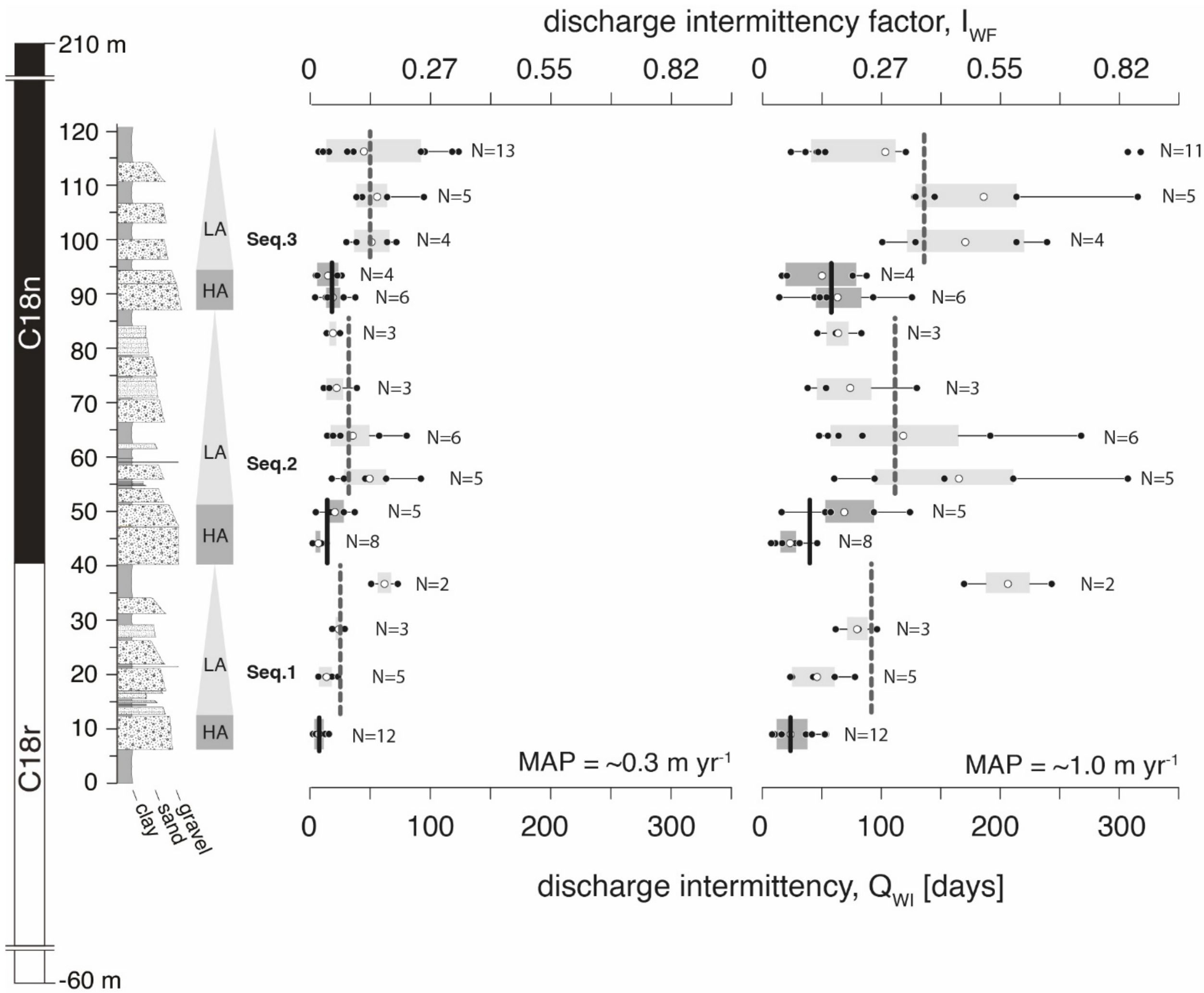

Figure 3. Discharge intermittency (Q_{WI}) and intermittency factor (I_{WF}) estimates from two end-members having MAP of ~ 300 mm yr^{-1}, and ~ 1000 mm yr^{-1}. Values are strongly dependent on precipitation rate such that the more water is available, the less intermittent the fluvial system becomes. Black vertical bars denote the average value in HA intervals while grey bars denote the average value in LA intervals.

Sediment flux estimates

Non-dimensional unit sediment flux, q_t (Eq. 1), based on the model of Engelund and Hansen (1967), was estimated to be 63.5 ± 21 (average value ± standard error, N = 35) for the HA intervals and 61 ± 20 (N = 49) for the LA intervals. This would imply bankfull sediment flux using the sand fraction (Eq. 4) for HA intervals to be 0.2 ± 0.06 m^3 s^{-1} and 0.1 ± 0.02 m^3 s^{-1} for the LA intervals, i.e., a 2-fold increase in sediment flux during HA intervals. This compares well to the 1.5-fold increase in bedload sediment flux in the HA intervals recently documented by Sharma et al. (2023) (Fig. 4).

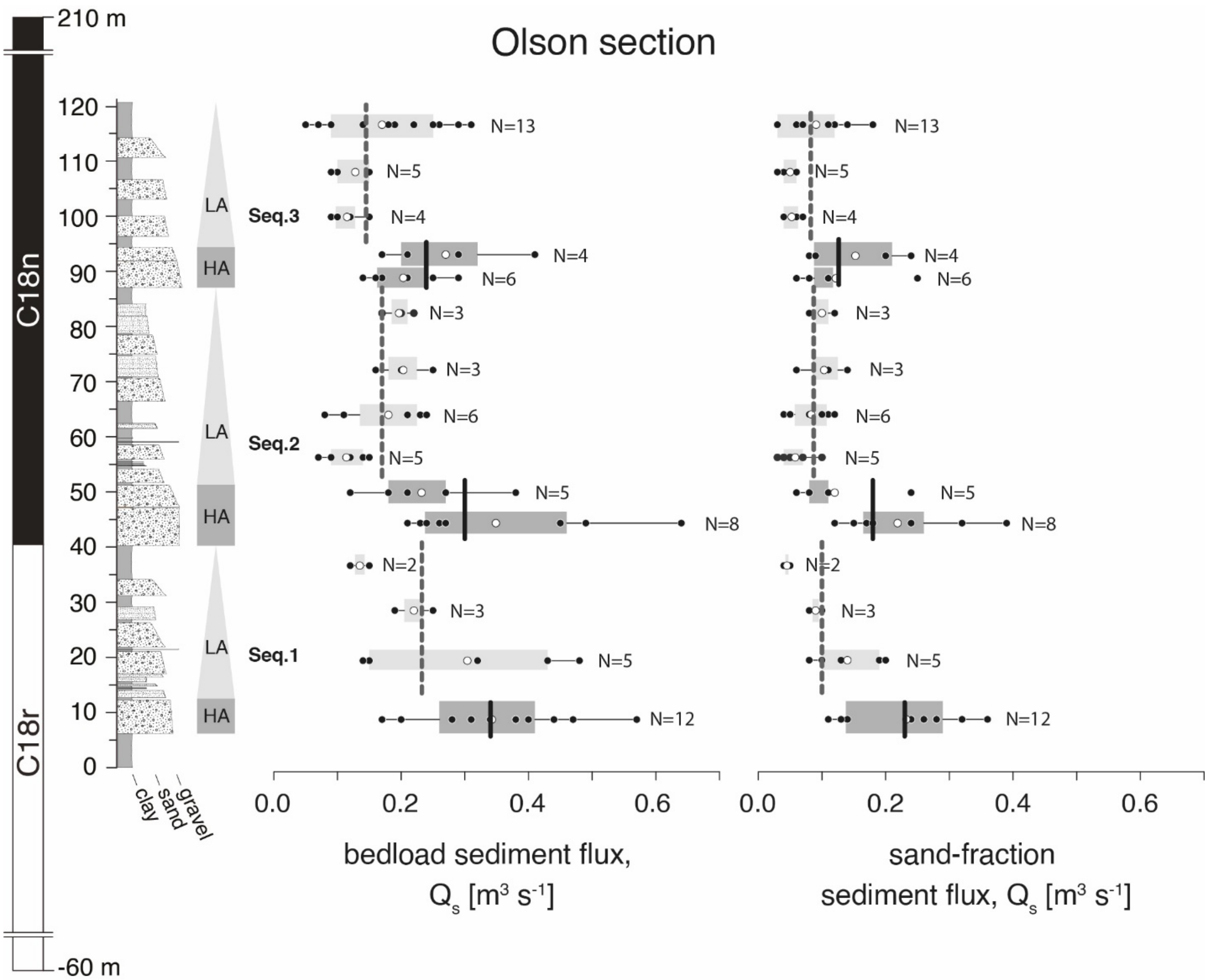

Figure 4. Bedload sediment flux calculated by Sharma et al. (2023), using the Meyer-Peter and Muller equation, and sand-fraction sediment flux calculated using the Engelund and Hansen (1967) model. Black vertical bars denote the average value in HA intervals while grey bars denote the average value in LA intervals.

Sediment flux intermittency factor (I_{SF})

Sediment flux intermittency, based on bedload flux, in the HA intervals is 3 ± 0.2 days (average value ± standard error, N = 35), equivalent to an intermittency factor of 0.008 or 0.8 % of a year, while LA intervals have an intermittency of 5 ± 0.4 days (N = 49), equivalent to an intermittency factor of 0.01 or 1 % of a year (Fig. 5).

Intermittency based on sand-fraction sediment flux, in the HA intervals is 5 ± 0.5 days (N = 35), intermittency factor of 0.01 (1 % of a year), while LA intervals have an intermittency of 11 ± 0.8 days (N = 49) i.e., an intermittency factor of 0.03 (3 % of a year) (Fig. 5). These data suggest that events moving sediment through the Escanilla system happened more intermittently than water transport and likely occurred on just a few days in a year. Again, HA intervals are reconstructed to have lower sediment flux intermittency factor (i.e., more intermittent sediment transport) than LA intervals.

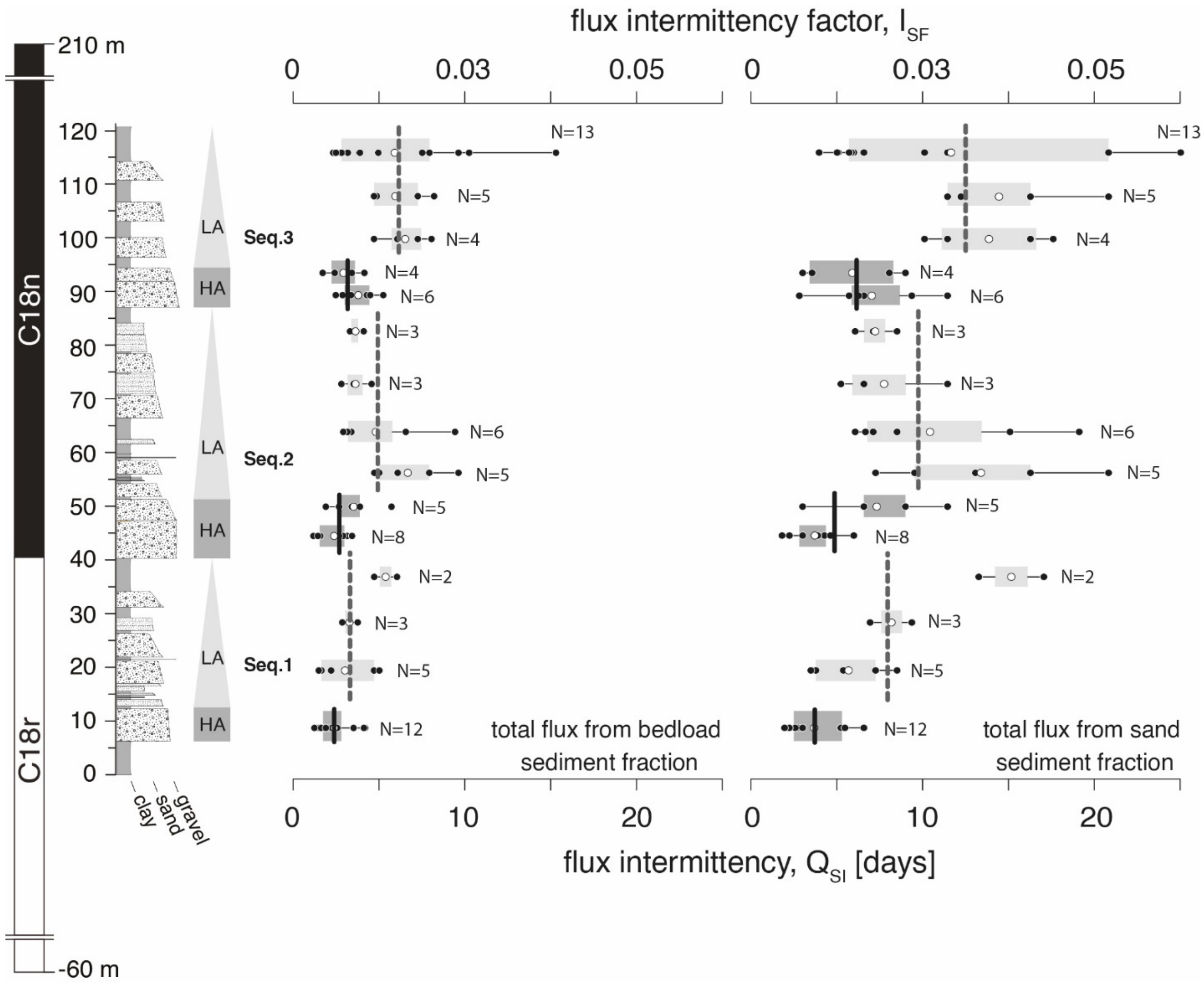

Figure 5. Sediment flux intermittency (Q_{SI}) and intermittency factor (I_{SF}) based on total flux estimated from bedload-fraction, and sand-fraction sediment flux. Black vertical bars denote the average value in HA intervals while grey bars denote the average value in LA intervals.

DISCUSSION

These results provide new insights into how water discharge and sediment transport evolved relative to alluvial channel stratal architecture in the Middle Eocene Escanilla Formation. We find that discharge and flux intermittency factor is systematically lower in HA intervals and higher in LA intervals (Fig. 3, 5). Given that we do not have evidence for very large changes in mean annual rainfall during this period (e.g., Fig. 2), we instead hypothesize these could be due to changes in the distribution of rainfall and storminess at these timescales.

According to paleogeographic reconstructions from Hay et al. (1999), the Pyrenees were situated approximately at 35° N during the Eocene period. This particular latitude is recognized to be vulnerable to climate changes induced by astronomical factors with some studies suggesting that orbital variations could impact precipitation and evaporation patterns at such latitudes [Cantalejo et al., 2014]. For instance, in the Middle Eocene (Late Lutetian) Ainsa System submarine fan deposits, cyclical variations in relatively coarser and finer-grained sediments reflects a strong relation to the 400-kyr eccentricity cycles [Cantalejo et al., 2014; 2020]. In the continental Escanilla Formation, 400-kyr eccentricity cycles have recently been proposed to influence sediment depositional patterns from HA to LA intervals due to cyclical variations in sediment flux and water discharge [Sharma et al., 2023].

These new intermittency results indicate that sediments during the deposition of HA intervals were on average transported within 4 days, most likely suggesting that HA intervals were deposited under concentrated 'bursts' of sediment flux probably under high-frequency convective storms over the Pyrenees during summertime [Callado and Pascual, 2005; Llasat et al., 2021], while sediment transport in LA intervals took on average 8 days but represent a much larger spread in the number of days over which sediments were transported (Fig. 5).

Collectively, this suggests a strong link between eccentricity cycles, discharge and flux rates, and their respective intermittencies in the Escanilla Formation such that eccentricity maxima most likely corresponds to higher flux and discharge, and potentially more stormy conditions that resulted in concentrated flow events (more intermittent flow) during the deposition of HA intervals. Contrary to this, eccentricity minima most likely corresponds to lower discharge and flux in the Escanilla system under calm climatic conditions with less intermittent flow conditions.

Sediment flux intermittency (I_{SF}) to water discharge intermittency (I_{WF}) ratio

For an MAP value of ~0.3 m yr^{-1}, the ratio of sediment flux intermittency factors (from bedload flux) to water discharge intermittency is 0.33 and 0.17 in the HA and LA intervals, i.e., 33% and 17% of the water discharge intermittency factor (Fig, 6). For the same MAP, the ratio of sediment flux intermittency factor (from sand fraction sediment flux) to water discharge intermittency factor is 0.52 and 0.43 in the HA and LA intervals, i.e., 52% and 43% of the water discharge intermittency factor (Fig. 6).

For an MAP value of ~1.0 m yr^{-1}, we obtain similar trends: 10% and 5% of the water discharge intermittency factor for HA and LA intervals (Fig. 6). And 16% and 13% of sediment flux intermittency for HA and LA intervals (Fig. 6).

This implies that sediment transport intermittencies vary in proportion to the assumed rainfall such that during lower rainfall rates, discharge and flux intermittency are similar in value since the infrequent discharge and sediment transport events happen together. However, as rainfall increases, the total water budget also increases resulting in flow events that do not transport any sediments. The resulting sediment transport intermittency factor, in this case, therefore, constitutes only a small proportion of the discharge intermittency factor.

These results also demonstrate how upstream environmental drivers (precipitation) can be predominant factor that determines how sediments are transported in fluvial systems and reinforces the idea that upstream climatic factors play an important role in how sediments are mobilized, and how they influence the resulting depositional architecture (c.f. Sharma et al. (2023)).

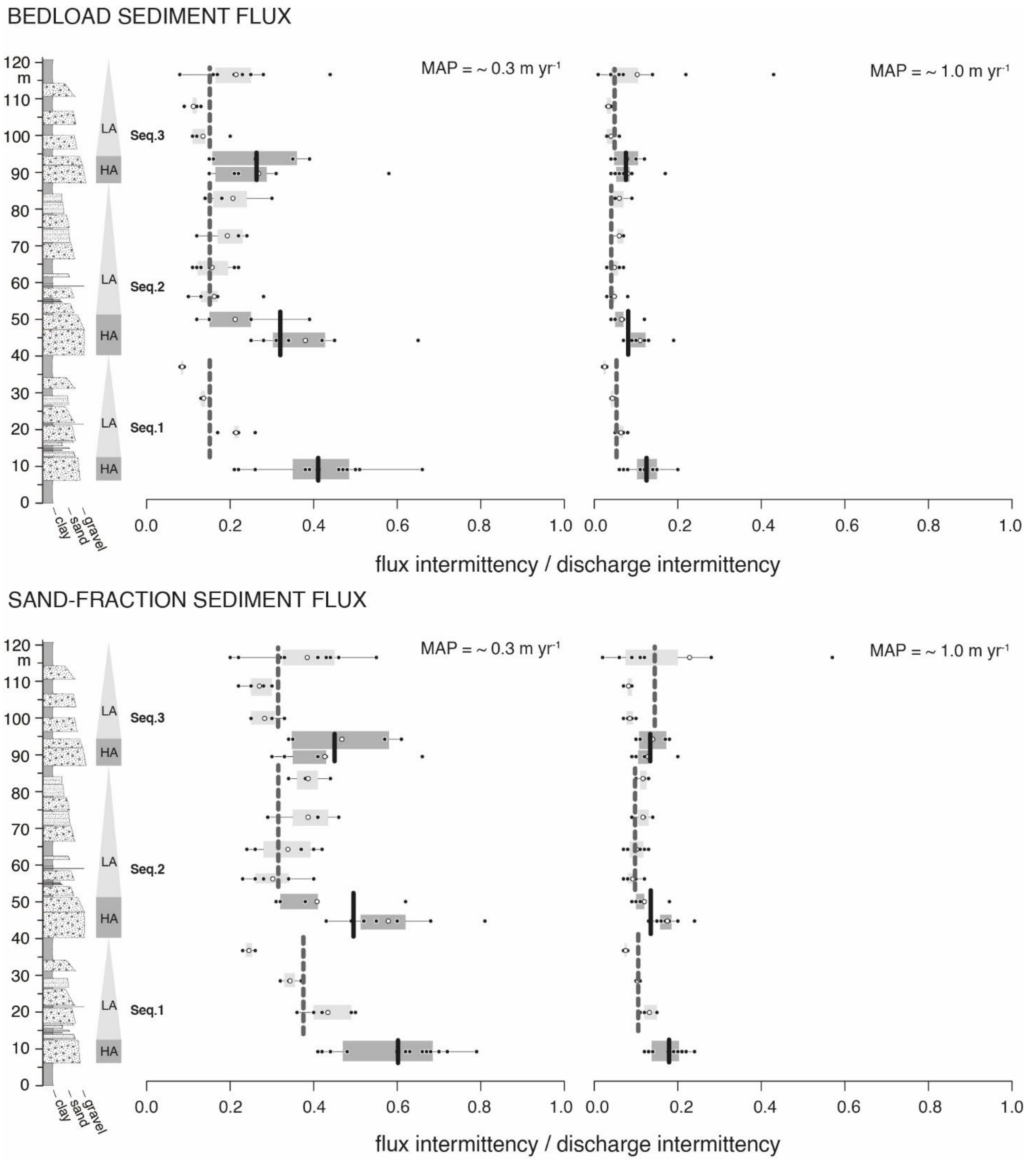

Figure 6. Ratio of sediment flux intermittency, based on bedload and sand-fraction flux estimates, and water discharge intermittency

How do our results compare to modern rivers?

To contextualize our findings, we compare them to the flux intermittency factor of 94 gravel bedded modern rivers, having grain size ranging from 0.003 – 0.08 m, with the flux intermittency factor from the HA and LA intervals deduced in this study (Fig. 6). Modern rivers from climatic environments with MAP ranging from 0.4 – 1.2 m yr^{-1} were selected from the dataset of Hayden et al. (2021) (see supplementary material).

Sediment flux intermittency factors of HA and LA intervals from the Escanilla Formation range from 0.008 to 0.03 with an average value of 0.02 (N = 82), while those from modern rivers have intermittency values ranging from 0.0026 to 0.8 with an average value of 0.14 (N = 94). These results suggest that our results are plausible and similar to sediment flux intermittency values of ephemeral rivers [Hayden et al., 2021]. It is also expected that sediment flux intermittency factors are lower than corresponding water intermittencies [Lyster et al., 2022] as not all real-world discharge conditions will transport sediment at maximum capacity.

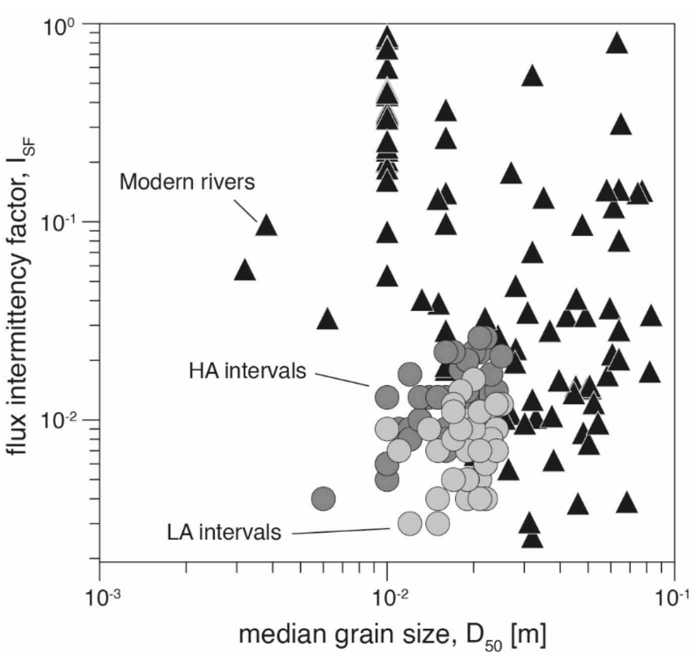

Figure 7. Comparison between flux intermittency factor of modern rivers (black triangles), and intermittent rivers (dark grey circles; HA intervals) and perennial rivers (light grey circles; LA intervals) from the Escanilla Formation, having the same median grain size range.

CONCLUSIONS

A quantitative approach of estimating discharge and flux variability relative to changes in fluvial stratigraphic architecture provides new insights into how channel stacking pattern in ancient sedimentary successions can be interpreted. Cyclical variations in discharge and flux intermittency correspond to changes in architectural styles such that HA intervals are deposited under more intermittent flow conditions (discharge intermittency of 12 – 40 days per year) which we interpret to be influenced by short and intense precipitation events while LA intervals are deposited under less intermittent flow conditions (discharge intermittency of 39 – 119 days per year). Overall, sediment flux intermittency factor of the Escanilla Formation has values ranging from 0.008 to 0.03 (3 – 11 days per year), which are within the same range of values from modern ephemeral rivers (0.0026 to 0.954). These values are typical of rivers found in arid and semi-arid climatic conditions and are consistent with the regional climate at Olson during the Middle Eocene. This further demonstrates the ability of paleohydraulic reconstructions to predict, within acceptable uncertainties, estimates that are consistent with values from modern rivers. Our data suggests that changes in depositional architectures are the result of relatively infrequent sediment transport events and indicate that changing rainfall distributions (as well as magnitudes) significantly influenced sediment routing systems on the Earth's surface in the past.

REFERENCES

1. Alexander, J., Fielding, C.R., Pocock, G.D. (1999) Flood behaviour of the Burdekin River, tropical north Queensland, Australia. In: Marriott, S.B., Alexander, J. (Eds.), Floodplains: Interdisciplinary Approaches. Geological Society of London, Special Publication 163, pp. 27–40.
2. Allemand, P., Lajeunesse, E., Devauchelle, O., Langlois, V.J. (2022) Entrainment and deposition of boulders in a gravel bed river. Earth Surf Dynam 11, 21–32. https://doi.org/10.5194/esurf-11-21-2023
3. Allen, J.P., Fielding, C.R., Rygel, M.C., Gibling, M.R. (2013) Deconvolving Signals of Tectonic and Climatic Controls From Continental Basins: An Example From the Late Paleozoic Cumberland Basin, Atlantic Canada. J Sediment Res 83, 847–872. https://doi.org/10.2110/jsr.2013.58
4. Armitage, J.J., Duller, R.A., Whittaker, A.C., and Allen, P.A. (2011) Transformation of tectonic and climatic signals from source to sedimentary archive: Nature Geoscience, v. 4, p. 231–235, doi:10.1038/ngeo1087.
5. Beaufort, A., Carreau, J., Sauquet, E. (2019) A classification approach to reconstruct local daily drying dynamics at headwater streams. Hydrol. Process. 33, 1896–1912. https://doi.org/10.1002/hyp.13445
6. Bentham, P.A., Burbank, D.W., and Puigdefabregas, C. (1992) Temporal and spatial controls on the alluvial architecture of an axial drainage system: late Eocene Escanilla Formation, southern Pyrenean foreland basin, Spain: Basin Research, v. 4, p. 335–352, doi:10.1111/j.1365-2117.1992.tb00052.x.
7. Bentham, P.A., Talling, P.J., and Burbank, D.W. (1993) Braided stream and flood-plain deposition in a rapidly aggrading basin: the Escanilla formation, Spanish Pyrenees: Geological Society, London, Special Publications, v. 75, p. 177–194, doi:10.1144/gsl.sp.1993.075.01.11.

8. Bentham, P.A., Talling, P.J., Burbank, D.W. (1993) Braided stream and flood-plain deposition in a rapidly aggrading basin: the Escanilla formation, Spanish Pyrenees. Geological Soc Lond Special Publ 75, 177–194. https://doi.org/10.1144/gsl.sp.1993.075.01.11
9. Blum, M.D., and Tornqvist, T.E. (2000) Fluvial responses to climate and sea-level change: a review and look forward: Sedimentology, v. 47, p—2--48, doi:10.1046/j.1365-3091.2000.00008.x.
10. Bond, N., McMaster, D., Reich, P., Thomson, J.R., Lake, P.S. (2010) Modelling the impacts of flow regulation on fish distributions in naturally intermittent lowland streams: an approach for predicting restoration responses. Freshwater Biol 55, 1997–2010. https://doi.org/10.1111/j.1365-2427.2010.02421.x
11. Brewer, C.J., Hampson, G.J., Whittaker, A.C., Roberts, G.G., Watkins, S.E. (2020) Comparison of methods to estimate sediment flux in ancient sediment routing systems. Earth-sci Rev 207, 103217. https://doi.org/10.1016/j.earscirev.2020.103217
12. Buttle, J.M., Boon, S., Peters, D.L., Spence, C., Meerveld, H.J. (Ilja) van, Whitfield, P.H. (2012) An Overview of Temporary Stream Hydrology in Canada. Can Water Resour J Revue Can Des Ressources Hydriques 37, 279–310. https://doi.org/10.4296/cwrj2011-903
13. Cabré, S.P. et al. (2023) Fluvio-deltaic record of increased sediment transport during the Middle Eocene Climatic Optimum (MECO), Southern Pyrenees, Spain: Climate of the Past, v. 19, p. 533–554, doi:10.5194/cp-19-533-2023.
14. Callado, A., Pascual, R. (2005) Diagnosis and modelling of a summer convective storm over Mediterranean Pyrenees. Adv Geosciences 2, 273–277. https://doi.org/10.5194/adgeo-2-273-2005
15. Cantalejo, B., and Pickering, K.T. (2014) Climate forcing of fine-grained deep-marine systems in an active tectonic setting: Middle Eocene, Ainsa Basin, Spanish Pyrenees:

Palaeogeography, Palaeoclimatology, Palaeoecology, v. 410, p. 351–371, doi:10.1016/j.palaeo.2014.06.005.

16. Cantalejo, B., Pickering, K.T., Miller, K.G., and Niocaill, C.M. (2021) Chasing the 400 kyr pacing of deep-marine sandy submarine fans: Middle Eocene Aínsa Basin, Spanish Pyrenees: Journal of the Geological Society, v. 178, p. jgs2019-173, doi:10.1144/jgs2019-173.
17. Castelltort, S., and Driessche, J.V.D. (2003) How plausible are high-frequency sediment supply-driven cycles in the stratigraphic record? Sedimentary Geology, v. 157, p. 3–13, doi:10.1016/s0037-0738(03)00066-6.
18. Costigan, K. H., Kennard, M. J., Leigh, C., Sauquet, E., Datry, T., & Boulton, A. J. (2017) Chapter 2—2 - flow regimes in intermittent Rivers and ephemeral streams. In T. Datry, N. Bonada, & A. Boulton (Eds.), Intermittent Rivers and ephemeral streams (pp. 51–78). Academic Press.
19. Dreyer, T. (1993) Quantified Fluvial Architecture in Ephemeral Stream Deposits of the Esplugafreda Formation (Palaeocene), Tremp-Graus Basin, Northern Spain. In: Alluvial Sedimentation (*Wiley*).
20. Dreyer, T., Fält, L. -M., Høy, T., Knarud, R., Steel§, R., and Cuevas, J. -L. (1992) The Geological Modelling of Hydrocarbon Reservoirs and Outcrop Analogues: , p. 57–80, doi:10.1002/9781444303957.ch3.
21. Eide, C.H., Müller, R., and Helland-Hansen, W. (2018) Using climate to relate water discharge and area in modern and ancient catchments: Sedimentology, v. 65, p. 1378–1389, doi:10.1111/sed.12426.
22. Eide, C.H., Müller, R., Helland-Hansen, W. (2018) Using climate to relate water discharge and area in modern and ancient catchments. Sedimentology 65, 1378–1389. https://doi.org/10.1111/sed.12426

23. Eng, K., Wolock, D.M., Dettinger, M.D. (2016) Sensitivity of Intermittent Streams to Climate Variations in the USA. River Res Applic 32, 885–895. https://doi.org/10.1002/rra.2939
24. Engelund, F., & Hansen, E. (1967). A monograph on sediment transport in alluvial streams (Vol. 4). Tekniskforlag Skelbrekgade.
25. Fielding, C.R., Alexander, J., Allen, J.P. (2018) The role of discharge variability in the formation and preservation of alluvial sediment bodies. Sediment Geol 365, 1–20. https://doi.org/10.1016/j.sedgeo.2017.12.022
26. Fielding, C.R., Allen, J.P., Alexander, J., Gibling, M.R. (2009) Facies model for fluvial systems in the seasonal tropics and subtropics. Geology 37, 623–626. https://doi.org/10.1130/g25727a.1
27. Fielding, C.R., Allen, J.P., Alexander, J., Gibling, M.R., Rygel, M.C., Calder, J.H. (2011) From River to Rock Record: The preservation of fluvial sediments and their subsequent interpretation. https://doi.org/10.2110/sepmsp.097.089
28. Fovet, O., Belemtougri, A., Boithias, L., Braud, I., Charlier, J., Cottet, M., Daudin, K., Dramais, G., Ducharne, A., Folton, N., Grippa, M., Hector, B., Kuppel, S., Coz, J.L., Legal, L., Martin, P., Moatar, F., Molénat, J., Probst, A., Riotte, J., Vidal, J., Vinatier, F., Datry, T. (2021) Intermittent rivers and ephemeral streams: Perspectives for critical zone science and research on socio-ecosystems. Wiley Interdiscip Rev Water 8. https://doi.org/10.1002/wat2.1523
29. Hansford, M.R., Plink-Björklund, P. (2020) River discharge variability as the link between climate and fluvial fan formation. Geology 48, 952–956. https://doi.org/10.1130/g47471.1
30. Hansford, M.R., Plink-Björklund, P., Jones, E.R. (2019) Global quantitative analyses of river discharge variability and hydrograph shape with respect to climate types. Earth-sci Rev 200, 102977. https://doi.org/10.1016/j.earscirev.2019.102977

31. Kjemperud, A.V., Schomacker, E., Brendsdal, A., Fält, L.-M., Jahren, J.S., Nystuen, J.P., and Puigdefàbregas, C. (2004) The Fluvial Analogue Escanilla Formation, Ainsa Basin, Spanish Pyrenees: Revisited: Search and Discovery, https://www.searchanddiscovery.com/documents/2004/kjemperud/.
32. Labourdette, R. (2011) Stratigraphy and static connectivity of braided fluvial deposits of the lower Escanilla Formation, south central Pyrenees, Spain: AAPG Bulletin, v. 95, p. 585–617, doi:10.1306/08181009203.
33. Labourdette, R. (2011) Stratigraphy and static connectivity of braided fluvial deposits of the lower Escanilla Formation, south central Pyrenees, Spain. Aapg Bull 95, 585–617. https://doi.org/10.1306/08181009203
34. Labourdette, R., Jones, R.R. (2007) Characterization of fluvial architectural elements using a three-dimensional outcrop data set: Escanilla braided system, South-Central Pyrenees, Spain. Geosphere 3, 422–434. https://doi.org/10.1130/ges00087.1
35. Lague, D., Hovius, N., Davy, P. (2005) Discharge, discharge variability, and the bedrock channel profile. J Geophys Res Earth Surf 110, n/a-n/a. https://doi.org/10.1029/2004jf000259
36. Langbein, W.B., Schumm, S.A. (1958) Yield of sediment in relation to mean annual precipitation. Eos Transactions Am Geophys Union 39, 1076–1084. https://doi.org/10.1029/tr039i006p01076
37. Llasat, M.C., Moral, A. del, Cortès, M., Rigo, T. (2021) Convective precipitation trends in the Spanish Mediterranean region. Atmos Res 257, 105581. https://doi.org/10.1016/j.atmosres.2021.105581
38. Lyster, Sinead and Whittaker, Alexander and Farnsworth, Alex and Hampson, Gary. (2022). Constraining flow and sediment transport intermittency in the geological past. 10.31223/X5S93S.

39. Mabbutt, J. (1977) Desert Landforms: An Introduction to Systematic Geomorphology. MIT Press, Massachusetts.

40. Matthews, W.J. (1988) North American Prairie Streams as Systems for Ecological Study. J N Am Benthol Soc 7, 387–409. https://doi.org/10.2307/1467298

41. Michael, N.A., Carter, A., Whittaker, A.C., and Allen, P.A. (2014b) Erosion rates in the source region of an ancient sediment routing system: comparison of depositional volumes with thermochronometric estimates: Journal of the Geological Society, v. 171, p. 401–412, doi:10.1144/jgs2013-108.

42. Michael, N.A., Whittaker, A.C., and Allen, P.A. (2013) The Functioning of Sediment Routing Systems Using a Mass Balance Approach: Example from the Eocene of the Southern Pyrenees: The Journal of Geology, v. 121, p. 581–606, doi:10.1086/673176.

43. Michael, N.A., Whittaker, A.C., Carter, A., and Allen, P.A. (2014a) Volumetric budget and grain-size fractionation of a geological sediment routing system: Eocene Escanilla Formation, south-central Pyrenees: GSA Bulletin, v. 126, p. 585–599, doi:10.1130/b30954.1.

44. Pancost, R.D. (2017) Climate change narratives: Nature Geoscience, v. 10, p. 466–468, doi:10.1038/ngeo2981.

45. Paola, C., Heller, P.L., Angevine, C.L. (1992) The large-scale dynamics of grain-size variation in alluvial basins, 1: Theory. Basin Res 4, 73–90. https://doi.org/10.1111/j.1365-2117.1992.tb00145.x

46. Parsons, A.J., Michael, N.A., Whittaker, A.C., Duller, R.A., Allen, P.A. (2012) Grain-size trends reveal the late orogenic tectonic and erosional history of the south–central Pyrenees, Spain. J Geol Soc London 169, 111–114. https://doi.org/10.1144/0016-76492011-087

47. Phillips, C.B., Hill, K.M., Paola, C., Singer, M.B., Jerolmack, D.J. (2018) Effect of Flood Hydrograph Duration, Magnitude, and Shape on Bed Load Transport Dynamics. Geophys Res Lett 45, 8264–8271. https://doi.org/10.1029/2018gl078976

48. Phillips, C.B., Jerolmack, D.J. (2014) Dynamics and mechanics of bed-load tracer particles. Earth Surf Dynam 2, 513–530. https://doi.org/10.5194/esurf-2-513-2014
49. Picard, M.D., High, L.R. (1973) Sedimentary Structures of Ephemeral Streams. Developments in Sedimentology 17. Elsevier, Amsterdam, pp. 223 pp.
50. Picard, M.D., High, L.R. (1973) Sedimentary Structures of Ephemeral Streams. Developments in Sedimentology 17. Elsevier, Amsterdam, pp. 223 pp.
51. Plink-Björklund, P. (2015) Morphodynamics of rivers strongly affected by monsoon precipitation: Review of depositional style and forcing factors. Sediment Geol 323, 110–147. https://doi.org/10.1016/j.sedgeo.2015.04.004
52. Plink-Björklund, P. (2017) Latitudinal Controls on River Systems: Implications of Precipitation Variability 108. SEPM Special Publication, pp. 2–21. https://doi.org/10.2110/sepmsp.108.02
53. Poff, N. (1996) A hydrogeography of unregulated streams in the United States and an examination of scale-dependence in some hydrological descriptors. Freshwater Biol 36, 71–79. https://doi.org/10.1046/j.1365-2427.1996.00073.x
54. Romans, B.W., Castelltort, S., Covault, J.A., Fildani, A., and Walsh, J.P. (2016) Environmental signal propagation in sedimentary systems across timescales: Earth-Science Reviews, v. 153, p. 7–29, doi:10.1016/j.earscirev.2015.07.012.
55. Sauquet, E., Shanafield, M., Hammond, J.C., Sefton, C., Leigh, C., Datry, T. (2021) Classification and trends in intermittent river flow regimes in Australia, northwestern Europe and USA: A global perspective. J Hydrol 597, 126170. https://doi.org/10.1016/j.jhydrol.2021.126170
56. Sharma, N., Spangenberg, J.E., Adatte, T., Vennemann, T., Kocsis, L., Vérité, J., Valero, L., Castelltort, S. (2023) Middle Eocene Climatic Optimum (MECO) and its imprint in the continental Escanilla Formation, Spain. EGUsphere 2023, 1–25. https://doi.org/10.5194/egusphere-2023-894

57. Sharma, N., Whittaker, A., Watkins, S., Valero, L., Vérité, J., Puigdefàbregas, C., Adatte, T., Garces, M., Guillocheau, F. and Castelltort, S. (2022) December. Climate Controlled Fluvial Stratigraphic Architecture in the Middle Eocene Escanilla Formation, South-Central Pyrenees, Spain. In American Geophysical Union, Fall Meeting 2022 (AGU 2022) (pp. EP56A-02).
58. Sharma, N., Whittaker, A.C., Watkins, S.E., Valero, L., Vérité, J., Puigdefabregas, C., Adatte, T., Garcés, M., Guillocheau, F., Castelltort, S. (2023) Water discharge variations control fluvial stratigraphic architecture in the Middle Eocene Escanilla formation, Spain. Sci Rep 13, 6834. https://doi.org/10.1038/s41598-023-33600-6
59. Simpson, G., and Castelltort, S. (2012) Model shows that rivers transmit high-frequency climate cycles to the sedimentary record: Geology, v. 40, p. 1131–1134, doi:10.1130/g33451.1.
60. Syvitski, J.P.M., Milliman, J.D. (2007) Geology, Geography, and Humans Battle for Dominance over the Delivery of Fluvial Sediment to the Coastal Ocean. J Geology 115, 1–19. https://doi.org/10.1086/509246
61. Tardif, D., Toumoulin, A., Fluteau, F., Donnadieu, Y., Hir, G.L., Barbolini, N., Licht, A., Ladant, J.-B., Sepulchre, P., Viovy, N., Hoorn, C., Dupont-Nivet, G. (2021) Orbital variations as a major driver of climate and biome distribution during the greenhouse to icehouse transition. Sci Adv 7, eabh2819. https://doi.org/10.1126/sciadv.abh2819
62. Tofelde, S., Bernhardt, A., Guerit, L., and Romans, B.W. (2021) Times Associated With Source-to-Sink Propagation of Environmental Signals During Landscape Transience: Frontiers in Earth Science, v. 9, p. 628315, doi:10.3389/feart.2021.628315.
63. Tunbridge, I.P. (1981) Sandy high-energy flood sedimentati—n - some criteria for recognition, with an example from the Devonian of S.W. England. Sediment. Geol. 28, 79–95.

64. Vincent, S.J. (2001) The Sis palaeovalley: a record of proximal fluvial sedimentation and drainage basin development in response to Pyrenean mountain building. Sedimentology 48, 1—5--1276. https://doi.org/10.1046/j.1365-3091.2001.00421.x
65. Whittaker, A.C., Duller, R.A., Springett, J., Smithells, R.A., Whitchurch, A.L., Allen, P.A. (2011) Decoding downstream trends in stratigraphic grain size as a function of tectonic subsidence and sediment supply. Geol Soc Am Bull 123, 1363–1382. https://doi.org/10.1130/b30351.1
66. William W. Hay, Robert M. DeConto, Christopher N. Wold, Kevin M. Wilson, Silke Voigt, Michael Schulz, Adrienne Rossby Wold, Wolf-Christian Dullo, Alexander B. Ronov, Alexander N. Balukhovsky, Emanuel Söding (1999) "Alternative global Cretaceous paleogeogra”hy", Evolution of the Cretaceous Ocean-Climate System, Enriqueta Barrera, Claudia C. Johnson.

Acknowledgements

We thank the Swiss National Science Foundation for funding this work (SNSF Grant No. 200020_182017: Earth Surface Signaling Systems 2).

Author contributions

S.C. designed the project and obtained funding. N.S. computed, interpreted results, and wrote the manuscript with inputs from A.C.W., T.A. and S.C. A.C.W., T.A. and S.C. reviewed and provided comments on the manuscript.

Competing interests

The authors declare no competing interests.

Data availability

All data generated and analyzed in this study has been provided as supplementary material files accompanying this manuscript.